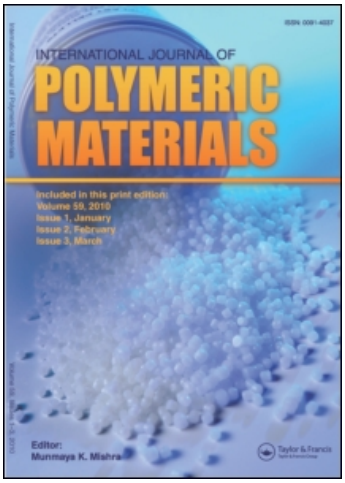

International Journal of Polymeric Materials
Publication details, including instructions for authors and subscription information:
http://www.informaworld.com/smpp/title~content=t713647664

Generating Line Spectra from Experimental Responses. III. Interconversion between Relaxation and Retardation Behavior

N. W. Tschoegl[ab]; I. Emri[ab]
[a] Division of Chemistry and Chemical Engineering, California Institute of Technology, Pasadena, California [b] Department of Mechanical Engineering, University of Ljubljana, Ljubljana, Slovenia

To cite this Article Tschoegl, N. W. and Emri, I.(1992) 'Generating Line Spectra from Experimental Responses. III. Interconversion between Relaxation and Retardation Behavior', International Journal of Polymeric Materials, 18: 1, 117 — 127
To link to this Article: DOI: 10.1080/00914039208034818
URL: http://dx.doi.org/10.1080/00914039208034818

Intern. J. Polymeric Mater., 1992, Vol. 18, pp. 117–127
Reprints available directly from the publisher
Photocopying permitted by license only

Printed in Great Britain

Generating Line Spectra from Experimental Responses. III. Interconversion between Relaxation and Retardation Behavior

N. W. TSCHOEGL and I. EMRI

Division of Chemistry and Chemical Engineering, California Institute of Technology, Pasadena, California 91125, and Department of Mechanical Engineering, University of Ljubljana, Ljubljana, Slovenia

(Received March 10, 1992)

An algorithm is described which allows relaxation line spectra to be interconverted into retardation line spectra, and *vice versa*. The first line spectrum is generated from a given experimental response such as the relaxation modulus, the storage modulus, or the loss modulus, or from a response such as the creep compliance, storage compliance, or loss compliance. The interconversion algorithm is here applied to the standard linear solid and liquid models, and to a 32-line spectrum simulating the behavior of an entangled polymer.

KEY WORDS Relaxation spectra, retardation spectra.

INTRODUCTION

In two previous publications[1,2] we have described three computer algorithms which generate the discrete relaxation spectrum

$$H(\tau) = \sum_{i=1}^{i=N} G_i\tau_i\delta(\tau_i - \tau) \tag{1}$$

from experimental data on either the relaxation modulus, $G(t)$, the storage modulus, $G'(\omega)$, or the loss modulus, $G''(\omega)$, or produce the discrete retardation spectrum

$$L(\tau) = \sum_{i=1}^{i=N} J_i\tau_i\delta(\tau_i - \tau) \tag{2}$$

from experimental data of either the creep compliance, $J(t)$, the storage compliance, $J'(\omega)$, or the loss compliance, $J''(\omega)$. The line spectra generated by these

algorithms faithfully reproduce the original input. Once the set of parameters $\{G_i, \tau_i\}$ is known, $G(t)$, $G'(\omega)$, or $G''(\omega)$ can be obtained from it using the relations

$$G(t) = \{G_e\} + \sum_{i=1}^{i=N} G_i \exp(-t/\tau_i), \tag{3}$$

$$G'(\omega) = \{G_e\} + \sum_{i=1}^{i=N} G_i \frac{\omega^2\tau_i^2}{1 + \omega^2\tau_i^2}, \tag{4}$$

and

$$G''(\omega) = \sum_{i=1}^{i=N} G_i \frac{\omega\tau_i}{1 + \omega^2\tau_i^2}. \tag{5}$$

Similarly, once the set $\{J_i, \tau_i\}$ has been obtained, $J(t)$, $J'(\omega)$, or $J''(\omega)$ can be recovered from

$$J(t) = J_g + \sum_{i=1}^{i=N} J_i[1 - \exp(-t/\tau_i)] + \{\phi_f t\}, \tag{6}$$

$$J'(\omega) = J_g + \sum_{i=1}^{i=N} J_i \frac{1}{1 + \omega^2\tau_i^2}, \tag{7}$$

and

$$J''(\omega) = \sum_{i=1}^{i=N} J_i \frac{\omega\tau_i}{1 + \omega^2\tau_i^2} + \{\phi_f/\omega\}. \tag{8}$$

In these equations G_e is the equilibrium modulus, G_g and J_g are the glassy modulus and compliance respectively, and ϕ_f is the steady-flow fluidity. The braces signify that $\{G_e\} = 0$, and $\{\phi_f t\} = \phi_f t$, $\{\phi_f/\omega\} = \phi_f/\omega$, when the material is *rheodictic*,[3a] i.e. exhibits steady-state flow, while $\{G_e\} = G_e$, and $\{\phi_f t\} = \{\phi_f/\omega\} = 0$, when the material is *arrheodictic*,[3a] i.e. does not exhibit steady-state flow.

THEORY

In this paper we develop a conversion algorithm which permits us to interconvert the sets $\{G_i, \tau_i\}$ and $\{J_i, \tau_i\}$. The interconversion[3b] utilizes the reciprocity between the *relaxance*,[3c]

$$\tilde{Q}(s) = G_g - \sum_{i=1}^{i=N} G_i \frac{1}{1 + \tau_i s}, \tag{9}$$

and the *retardance*[3c]

$$\bar{U}(s) = Jg + \sum_{i=1}^{i=N} J_i \frac{1}{1 + \tau_i s} + \{\phi_f/s\}. \tag{10}$$

$\bar{Q}(s)$ and $\bar{U}(s)$ are the Laplace transforms of the material's response to a unit impulse of strain, and of stress, respectively, s being the Laplace transform variable. They are linked through the simple relation[3d] $\bar{Q}(s)\bar{U}(s) = 1$. Because of the reciprocity between $\bar{Q}(s)$ and $\bar{U}(s)$, if the discrete relaxation spectrum, $H(\tau)$, has already been obtained, we may generate $\bar{Q}(s)$ from $\{G_i, \tau_i\}$, take its inverse at as many points as is necessary, and then apply the algorithm to be discussed below to this set of data to obtain the set $\{J_i, \tau_i\}$, i.e. the line spectrum, $L(\tau)$. Analogously, we may, of course, obtain $H(\tau)$, i.e. $\{G_i, \tau_i\}$, if we already have $L(\tau)$, i.e. $\{J_i, \tau_i\}$.

As in the two preceding papers,[1,2] we must now consider the span of the Boundary Window or Window 1, and that of the Modeling Window or Window 2. Window 1 determines the maximum allowable width for the region from which the algorithm selects datum points for the calculation of each successive spectrum line. Window 2 is the window within which the algorithm operates most efficiently when the number of spectrum lines exceeds 1 per decade. The kernel, $1/(1 + \tau s)$, is again a half-lorentzian, as is the storage kernel $1/(1 + \omega^2\tau^2)$. As shown in Figure 1, Window 1 ranges from $\log \tau s = -0.5$ to $\log \tau s = 0.5$.

Figure 2 shows the negative inverse of the first logarithmic derivative of the spectral kernel defined by

$$D_{\text{spec}} = \frac{d}{d \log \tau s}\left(\frac{1}{1 + \tau s}\right) = -\frac{2.303\,\tau s}{(1 + \tau s)^2}, \tag{11}$$

for three neighboring spectrum lines, and the width of Window 2 as given by the intersection of the lines. As a function of the number, n, of preselected spectrum lines per logarithmic decade it is again calculated as outlined in our earlier papers.[1,2]

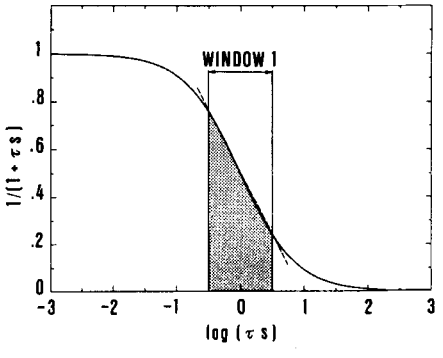

FIGURE 1 The kernel $1/(1 + \tau s)$ and Window 1.

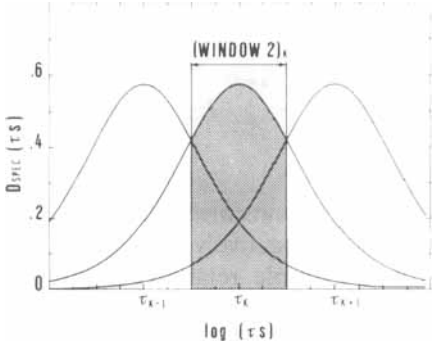

FIGURE 2 First derivatives of three neighboring spectrum lines and Window 2.

TABLE I

Lower and Upper Limits of Window 2 as Functions of n

n	$\log s_l\tau_k$	$\log s_u\tau_k$	n	$\log s_l\tau_k$	$\log s_u\tau_k$
1	−0.50	0.50	5	−0.10	0.10
2	−0.30	0.30	6	−0.08	0.08
3	−0.17	0.17	7	−0.07	0.07
4	−0.13	0.13	8	−0.06	0.06

We obtain the lower and upper limits of Window 2, s_l, and s_u, as functions of n from the equations

$$s_l^2 = \frac{\tau_k - \tau_{k+1}}{\tau_k^2\tau_{k+1} - \tau_{k+1}^2\tau_k} = \frac{1 - 10^{-1/n}}{10^{1/n} - 1}\frac{1}{\tau_k^2} \tag{12}$$

and

$$s_u^2 = \frac{\tau_k - \tau_{k+1}}{\tau_k^2\tau_{k+1} - \tau_{k+1}^2\tau_k} = \frac{10^{1/n} - 1}{1 - 10^{-1/n}}\frac{1}{\tau_k^2}. \tag{13}$$

For a single spectrum line the widths of Windows 1 and 2 coincide, as they did in the case of the exponential kernel,[1] and of the half-lorentzian and lorentzian kernels.[2] Since the kernel is self-congruent,[3c] the lower and upper limits are symmetric on the logarithmic scale. Values for $n = 1$ to $n = 8$ are tabulated in Table I.

THE CONVERSION ALGORITHM

We now describe our conversion algorithm for the case when we have determined $\{G_i, \tau_i\}$, and wish to obtain $\{J_i, \tau_i\}$. We begin by generating a discrete set of values $\{\bar{Q}_j, s_j; j = 1 \cdots M\}$ from Equation (9). These are then converted point by point

to the set $\{\bar{U}_j, s_j; j = 1 \cdots M\}$ using the relation $\bar{Q}(s)\bar{U}(s) = 1$. We then apply the algorithm to the normalized discrete retardance.

$$\hat{u}(s_j) = \frac{\bar{U}_j - \{\phi_f/s_j\}}{\bar{U}_1 - \{\phi_f/s_1\} - \bar{U}_M} = \hat{u}(s_M) + \sum_{i=1}^{i=N} \hat{j}_i \frac{1}{1 + \tau_i s}, \tag{14}$$

where the $\hat{j}_i$'s are the normalized compliances, J_i, and where[3f]

$$\phi_f = 1/\eta_f = \left(\sum_{i=1}^{i=N} G_i \tau_i\right)^{-1} \tag{15}$$

which is the expression* linking the steady-state fluidity, ϕ_f, to $\{G_i, \tau_i\}$.

We now separate out the kth spectrum line. This gives

$$\hat{u}(s_j) = \hat{u}(s_M) + \sum_{i=1}^{i=k-1} \hat{j}_i \frac{1}{1 + \tau_i s_j} + \hat{j}_k \frac{1}{1 + \tau_i s_j} + \sum_{i=k+1}^{i=N} \hat{j}_i \frac{1}{1 + \tau_i s_j} + \Delta_j \tag{16}$$

where $\Delta_j = \Delta_j^e + \Delta_j^a$ again account for any experimental or approximation error.[1,2]

The sum of squares of Δ_j within Window 2 is given by

$$E_k = \sum_{j=z_{k,l}}^{j=z_{k,u}} \Delta_j^2 \tag{17}$$

where $z_{k,l}$ and $z_{k,u}$ are the first and the last discrete points in the window which belongs to the kth spectrum line. Minimizing the error according to $\partial E_k/\partial \hat{j}_k = 0$, leads to

$$\hat{j}_k = \frac{\sum_{j=z_{k,l}}^{j=z_{k,u}} \Psi(s_j) \frac{1}{1 + \tau_k s_j}}{\sum_{j=z_{k,l}}^{j=z_{k,u}} \left(\frac{1}{1 + \tau_k s_j}\right)^2} \tag{18}$$

where

$$\Psi(s_j) = \hat{u}(s_j) - \hat{u}(s_M) - \sum_{i=1}^{i=k-1} \hat{j}_k \frac{1}{1 + \tau_i s_j} - \sum_{i=k+1}^{i=N} \hat{j}_k \frac{1}{1 + \tau_i s_j}. \tag{19}$$

Equations (18) and (19) constitute the algorithm for evaluating $\{J_j, \tau_j\}$ from $\{G_j, \tau_j\}$. If it is desired to find $\{G_j, \tau_j\}$ from $\{J_j, \tau_j\}$, then we have

$$\hat{q}(s_j) = \frac{\bar{Q}_j}{\bar{Q}_M - \bar{Q}_1} = \hat{q}(s_M) - \sum_{i=1}^{i=k-1} \hat{g}_i \frac{1}{1 + \tau_i s_j} - \hat{g}_k \frac{1}{1 + \tau_i s_j} - \sum_{i=k+1}^{i=N} \hat{g}_i \frac{1}{1 + \tau_i s_j} + \Delta_j. \tag{20}$$

*Equation (15) will give a satisfactory value only if the data span a sufficiently wide range of times or frequencies. Otherwise ϕ_f must be determined in other ways.

The minimization condition then yields

$$\hat{g}_k = \frac{\sum_{j=z_{k,l}}^{j=z_{k,u}} \Phi(s_j) \frac{1}{1 + \tau_k s_j}}{\sum_{j=z_{k,l}}^{j=z_{k,u}} \left(\frac{1}{1 + \tau_k s_j}\right)^2} \tag{21}$$

where

$$\Phi(s_j) = \hat{q}(s_M) - \hat{q}(s_j) - \sum_{i=1}^{i=k-1} \hat{g}_i \frac{1}{1 + \tau_i s_j} - \sum_{i=k+1}^{i=N} \hat{g}_i \frac{1}{1 + \tau_i s_j}. \tag{22}$$

RESULTS

For our first example to demonstrate the working of the conversion algorithm we selected the standard arrheodictic 3-parameter Maxwell model shown in Figure 3a for which

$$\bar{Q}(s) = G_g - \frac{G}{1 + \tau_M s}. \tag{23}$$

We generated $\bar{Q}(s)$ with the values $G_g = 10^9$, $G = 10^9/1.001$ N/m^2, and $\tau_M = 10^{-4}/1.001$ seconds. The model possesses a single spectrum line of strength G located at $\log \tau = \log \tau_M$. Both $\bar{Q}(s)$ and the line spectrum, $H(\tau)$, are shown in Figure 4.

Application of the conversion algorithm to $\bar{U}(s)$ as obtained from the relation $\bar{Q}(s)\bar{U}(s) = 1$ yielded a singlet spectrum. The line spectrum, $L(\tau)$, consisted in this case of a single line of strength $J = 10^{-6}$ m^2/N. This line was located at $\log \tau_V = -1$. It is also shown, together with $\bar{U}(s)$, in Figure 4.

It is readily shown that the algorithm did, indeed, furnish the correct value of the single line of the retardation spectrum. According to the linear theory of viscoelastic behavior,[3g] the standard arrheodictic 3-parameter Voigt model shown in Figure 3b, for which we have

$$\bar{U}(s) = J_g + \frac{J}{1 + \tau_V s}, \tag{24}$$

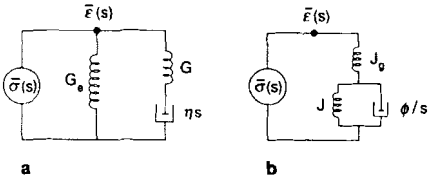

FIGURE 3 The 3-parameter Maxwell (3a), and Voigt (3b) models.

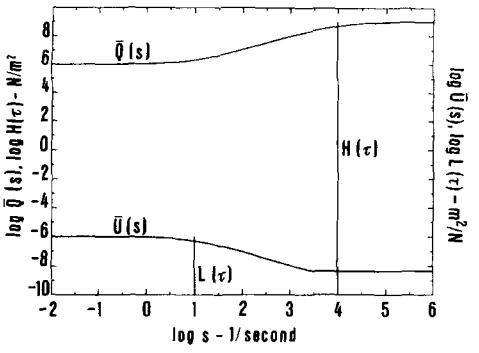

FIGURE 4 $\bar{Q}(s)$ and $\bar{U}(s)$ for the standard arrheodictic model as function of log s and the two lines representing the relaxation and retardation singlet spectra.

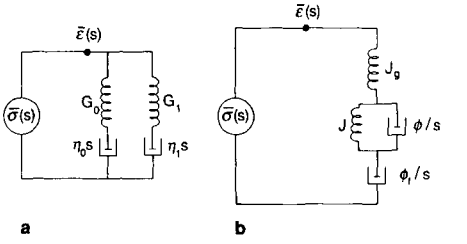

FIGURE 5 The 4-parameter Maxwell (5a) and Voigt (5b) models.

will exhibit identical behavior with that of the 3-parameter Maxwell model if the parameters of the two conjugate models are connected by the relations

$$J = G/G_g G_e \tag{25}$$

and

$$\tau_V = G_g \tau_M / G_e. \tag{26}$$

These relations are satisfied exactly. Expressed in other words, the algorithm has successfully converted the relaxation (line) spectrum, $H(\tau) = G\tau_M \delta(\tau_M - \tau)$, into the retardation (line) spectrum, $L(\tau) = J\tau_V \delta(\tau_V - \tau)$.

We obtained similar results with the rheodictic 4-parameter Maxwell model displayed in Figure 5a, for which

$$\bar{Q}(s) = G_g - \frac{G_0}{1 + \tau_0 s} - \frac{G_1}{1 + \tau_1 s}. \tag{27}$$

We constructed $\bar{Q}(s)$ this time with the parameters $G_0 = 10^6$, $G_1 = 10^9$ N/m^2, and $\tau_0 = 1$, $\tau_1 = 10^{-4}$ seconds. From this we obtained the two sets of datum points

$$\{\tilde{U}_j, s_j\} = 1/\{\tilde{Q}_j, s_j\} \tag{28}$$

and

$$\{\tilde{U}_j - \phi_f/s_j, s_j\} = \{\tilde{Q}_j^{-1} - \phi_f/s_j, s_j\}. \tag{29}$$

where $\phi_f = 1/(G_0 + G_1)$. These sets were plotted as connected lines in Figure 6.

Applying the conversion algorithm to the second set (which is corrected for the presence of the fluidity term), we obtained a doublet line spectrum. The locations of the two lines and their (normalized) strengths are listed in the first two rows of Table II.

To check the results obtained, we again turned to the theory of linear viscoelastic behavior. The Voigt model which is the conjugate[3h] of the 4-parameter Maxwell model is displayed in Figure 5b. Its retardance is given by

$$\tilde{U}(s) = J_g + \frac{J}{1 + \tau s} + \phi_f/s. \tag{30}$$

For the two models in Figure 5 to exhibit identical behavior, their parameters must be connected[3i] by the relations

$$J = \frac{G_0 G_1(\tau_1 - \tau_0)^2}{(G_0 + G_1)(G_0\tau_0 + G_1\tau_1)^2} \tag{31}$$

and

$$\tau_V = \frac{G_0 + G_1}{G_0/\tau_0 + G_1/\tau_1}. \tag{32}$$

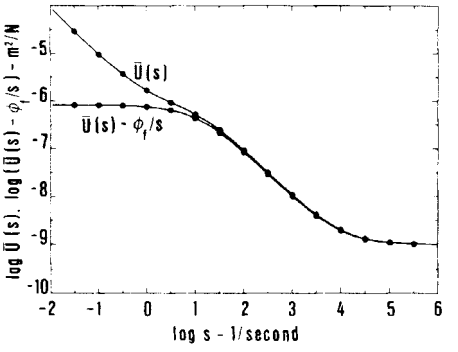

FIGURE 6 $\bar{U}(s)$ and $\bar{U}(s) - \phi/s$ obtained from the theoretical singlet spectrum and from the doublet spectrum furnished by the algorithm.

TABLE II

Calculated and True Values of Spectrum Lines

$J_1 = 0.9426$	$\tau_1 = 0.1000$
$J_2 = 0.0574$	$\tau_2 = 0.0316$
$J = 1.0000$	$\tau_V = 0.0910$

The appropriate values of J and of τ_V are listed in the third row of Table II. These values represent a singlet spectrum. Instead, the interconversion yielded a doublet spectrum. This is obtained, of course, because none of the locations of the algorithm's preselected spectrum lines coincide exactly with that of the 4-parameter Voigt model. The algorithm therefore places a large line at the preselected location nearest to that of the expected Voigt model line, and compensates for the mismatch by generating a second line. The effect of this on $\bar{U}(s)$ recovered from the doublet spectrum is extremely small. $\bar{U}(s)$ and $\bar{U}(s) - \phi/s$ calculated from

$$\bar{U}(s) = J_g + \frac{J_1}{1 + \tau_1 s} + \frac{J_2}{1 + \tau_2 s} + \phi_f/s, \tag{33}$$

and from Equation (30), are identical within the resolving power of a plot such as that shown in Figure 6 where the circles indicate the values calculated using the doublet spectrum. Incidentally, any discrepancies introduced because of the preselection of the spectral lines with which the algorithm operates can be decreased by increasing the number of lines per decade at the expense of a longer computer run time.

In our first two papers,[1,2] we demonstrated the power of the algorithm with the aid of a 32-line spectrum derived from a mathematical equation simulating the relaxation spectrum of an entangled, uncrosslinked, i.e. pseudo-arrheodictic,[3] polymer. The spectrum,

$$H(\tau) = \sum_{i=1}^{i=32} G_i \tau_i \delta(\tau_i - \tau), \tag{34}$$

is reproduced in Figure 7.

Figure 8 shows log $G(t)$ and log $\bar{Q}(s)$ calculated from this spectrum using Equations (3) and (9), respectively.

To derive the concomitant retardation spectrum, we proceeded essentially as with the standard rheodictic model. Using $\bar{Q}(s_j)$ we obtained $\bar{U}(s_j)$ by Equation (28) and $\bar{U}(s_j) - \phi_f/s_j$ by Equations (29) and (15). Each tenth point of these values is plotted as a full circle in Figure 10.

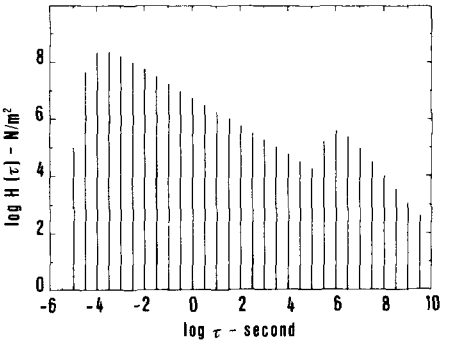

FIGURE 7 32-Line relaxation spectrum.

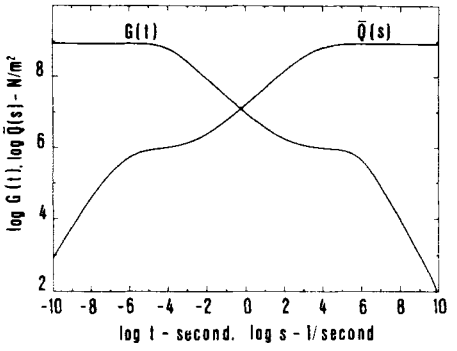

FIGURE 8 Log $G(t)$ and log $\bar{Q}(s)$ obtained from the 32-line relaxation spectrum.

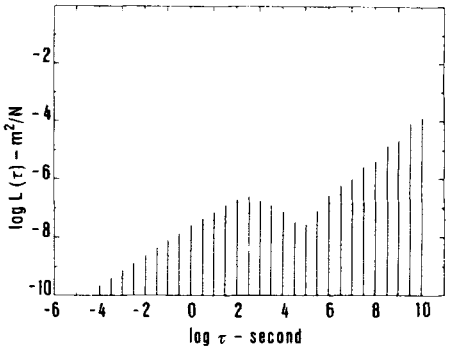

FIGURE 9 Retardation spectrum generated by the algorithm from the 32-line relaxation spectrum.

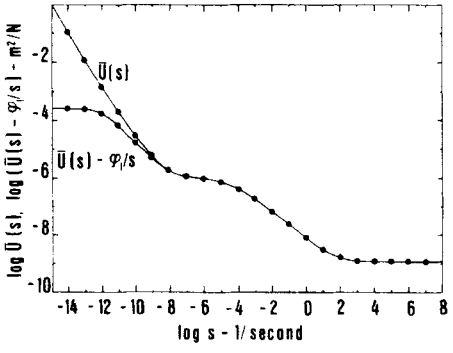

FIGURE 10 Log $\bar{U}(s)$ and log $[\bar{U}(s) - \phi_i/s]$ calculated from the retardation spectrum generated by the algorithm.

We then applied Equations (18) and (19) to obtain the retardation spectrum

$$L(\tau) = \sum_{i=1}^{i=32} J_i \tau_i \delta(\tau_i - \tau). \tag{32}$$

This is shown in Figure 9.

Figure 10 displays log $\tilde{U}(s)$ and log $[\tilde{U}(s) - \phi_f/s]$ calculated from Equation (10) using the parameters J_i and τ_i generated by the algorithm and are shown as solid lines. $\tilde{U}(s) - \phi_f/s$ clearly reveals the existence of the steady-state compliance J_e^0 at the left end of the curve.

CONCLUSIONS

The examples and illustrations adduced here satisfactorily demonstrate the viability of the interconversion algorithm. In a forthcoming publication[4] we intend to apply the algorithms discussed here and in the two preceding papers[1,2] to experimentally obtained data.

Acknowledgment

The authors gratefully acknowledge support of this work by the Slovene Ministry of Science under Grant P2-1131-782/91, and partial support by the California Institute of Technology.

References

1. I. Emri and N. W. Tschoegl, submitted to Rheol. Acta.
2. I. Emri and N. W. Tschoegl, submitted to Rheol. Acta.
3. N. W. Tschoegl, *The Phenomenological Theory of Linear Viscoelastic Behavior*. Springer-Verlag, Heidelberg, 1989; 3a: pp. 40 and 93; 3b: Sect. 8.1.1; 3c; p. 40; 3d: p. 42; 3e: p. 318; 3f: pp. 147 and 232; 3g: Sects. 3.4.1.1 and 3.7; 3h: p. 92; 3i: Sect. 3.7.
4. I. Emri and N. W. Tschoegl, submitted to Macromolecules.